

A mimic osseointegrated implant model for three-dimensional finite element analysis

Y. AKAGAWA, Y. SATO*, E. R. TEIXEIRA, N. SHINDOI & M. WADAMOTO *Department of Removable Prosthodontics, Hiroshima University Faculty of Dentistry, Kasumi, Hiroshima, Japan and *Department of Geriatric Dentistry, Showa University School of Dentistry, Tokyo, Japan*

SUMMARY The purpose of this study was to develop a new three-dimensional (3D) mimic model of an osseointegrated implant for finite element analysis (FEA) and to evaluate stress distributions in comparison with a model commonly used in most studies as a control. Based on the 3D computer graphic data obtained by serial *in vivo* bucco-lingual peri-implant bone structure at 75 µm interval in monkey, a mimic FEA model with trabecular structure and a control model with uniform cancellous bone were constructed. A vertical load of 143 N was applied at the top of the implant and induced stress was evaluated at the peri-implant bone. In the mimic model, stress was distributed at both cortical

and cancellous bones (1–5 MPa) in bucco-lingual central planes, but concentrated at the cortical crest (3–7 MPa) in the mesio-distal central plane. In contrast, the control model presented stress concentration at the cortical crest around the implant (5–14 MPa), with less stress (0–1 MPa) at the peri-implant cancellous bone in both planes. The findings, that stress distribution at the peri-implant bone were quite different between the mimic and control models, suggest the need to carefully interpret stress distribution in previous studies with models of uniform cancellous peri-implant bone.

KEYWORDS: 3D-FEA, implant, cancellous bone, mandible, monkey

Introduction

Biomechanics is one of the most important factors for the long-term stability of an osseointegrated implant, because mechanical stress by functional loading inevitably influences long-term peri-implant bone remodeling (Albrektsson, 1983; Hoshaw, Brunski & Cochran, 1994). Finite element analysis (FEA) has been widely applied to studies on stress distribution in the bone around the loaded osseointegrated implant and these studies show that induced stress by vertical and/or oblique loading is mostly concentrated at the crestal bone. This has led to the interpretation that such stress concentration in the bone is the most possible cause of crestal bone loss *in vivo* (Clelland *et al.*, 1991, 1995; Meijer *et al.*, 1993; Hoshaw *et al.*, 1994). However, such an interpretation appears to be premature, because little attention has been paid to the extent to which the modelling method significantly influences the results. In fact, the FEA models used in these studies do not well

represent peri-implant bone structure *in vivo*. Although it is shown that osseointegrated implants are surrounded by trabeculae in the cancellous bone area (Akagawa *et al.*, 1992; Wadamoto *et al.*, 1996), this trabecular peri-implant bone morphology was ignored and only 100% bone contact with a Young's modulus 10 times smaller than that of the cortical bone was assumed in most FEA studies (Holmes *et al.*, 1992, 1994; Meijer *et al.*, 1993, 1994). It is quite probable that these aspects of the FEA models lead to the finding of stress concentration at the crestal bone area. The detailed geometric representation of the object to be modelled influences the accuracy of an FEA (Korioth & Versluis, 1997). Therefore, it is hypothesized that stress distribution by loading may become more uniform at the crestal and cancellous bone area in a model with better representation of peri-implant cancellous bone structure.

The purpose of this study was first, to develop a new FEA model that represents the whole structure of the peri-implant cancellous bone, and secondly, to evaluate

our hypothesis by comparing stress distribution in this model with the model conventionally constructed with 100% bone contact used in most previous studies.

Materials and methods

Model construction

Three-dimensional (3D) FEA models were constructed based on the 3D graphic data of the bone around osseointegrated implants (Akagawa *et al.*, 1992; Wadamoto *et al.*, 1996). A block of mandible of a female adult monkey containing a plasma-sprayed hydroxyapatite-coated titanium alloy (Ti-6Al-4V*) fixture (3.6 mm in diameter, 8.0 mm in length) was obtained after 3 months of placement in the premolar edentulous region. This block was ground mesio-distally at 75 µm interval with the use of a grinding machine (Exakt Micro-Grinding System[†]). The ground surface was stained with toluidine blue and traced on a profile projector. Each traced bone structure was digitized and processed in a personal computer to yield the 3D graphics of the peri-implant bone and the implant (Fig. 1). Total bone contact ratio around whole surfaces was 68.8% (Wadamoto *et al.*, 1996). Subsequently, the voxel-based hexahedron meshing method was applied for model construction (Middleton, Jones & Pande, 1996). This object-oriented FEA modelling method involved a 300 µm cubic grid (Sato *et al.*, 1999b) superimposed on the object to be modelled, creating a 3D cubic element whenever the grid matches the object. To save calculation time and computer memory from the laboratory perspective, beam-type elements were applied to the outer planes of the model and 4.2 mm of bone at mesial and distal sides of the implant was found (Teixeira *et al.*, 1998). Each element was divided into four categories based on its own bone volume and the modified elastic property (Table 1) of each category followed by an assignment of bone volume (Fig. 2) (Sato *et al.*, 1999a). The model was a virtual representation of peri-implant bone structure and was termed the mimic model (MM) (elements: 32694; nodes: 42091) (Fig. 3).

Another model was constructed with similar dimensions for the MM and uniform cortical/cancellous bone structures with constant elastic properties (Table 1)

used in the previous studies (Holmes *et al.*, 1992, 1994; Meijer *et al.*, 1993, 1994). This was termed the control model (CM) (elements: 39536; nodes: 44397) (Fig. 3).

Analysis

Boundary fixation included restraints in all six degrees of freedom, involving rotation and translation in three coordinate axes for the correspondent nodes located at the most external mesial and distal planes in both models (Teixeira *et al.*, 1998). A vertical 143 N load (mean occlusal force of patients with osseointegrated-implant-supported bridges) (Brånemark, Zarb & Albrektsson, 1987) was applied to the top of the implant. Induced von Mises and principle stresses by loading were analysed with a personal computer (FMV Deskpower TE[‡]) and an FEA software program (Cosmos/M 1.75[§]).

Results

The von Mises stress in peri-implant bone in each model is shown in bucco-lingual and mesio-distal central planes (Fig. 4). A distinct difference in stress distribution was detected between MM and CM. In MM, stress was distributed in both cortical and cancellous bones in a range of 1–5 MPa. Slight concentration was seen around the apex of the implant (3–4 MPa) in the bucco-lingual central planes. In the mesio-distal central plane, stress was concentrated at the cortical crest (3–7 MPa) and was uniformly distributed in cancellous bone (1–4 MPa). In contrast, CM presented two- to three-times the amount of stress at the cortical crest around the implant (5–14 MPa) with less stress (0–1 MPa) distributed to the peri-implant cancellous bone. The principal stress indicated a distribution similar to the von Mises stress.

Discussion

In this study, a new mimic FEA model representing the whole structure of the peri-implant cancellous bone was developed and clear differences in stress distribution under loading were found. Uniform distribution at the cortical and cancellous bone areas was seen in this newly developed model. We believe this is the first

*Kyocera Inc., Kyoto, Japan.

†Exakt Apparatebau, Norderstedt, Germany.

‡Fujitsu, Tokyo, Japan.

§Structural Research and Analysis Corp., Santa Monica, CA, USA.

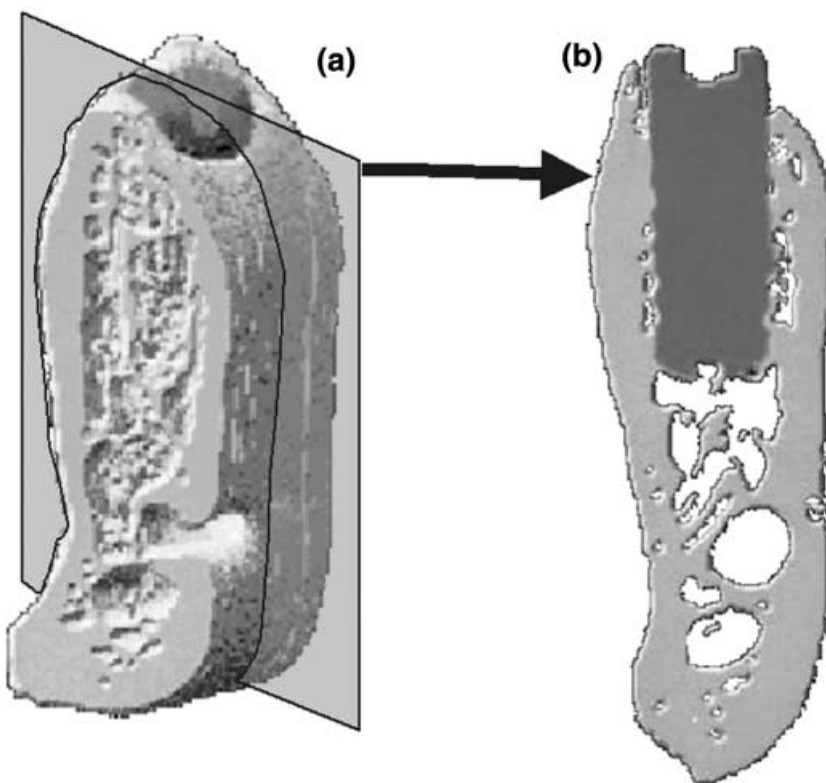


Fig. 1. Three dimensional graphics of the bone and the implant. (a) Oblique view, (b) Bucco-lingual central plane.

Table 1. Elastic properties assumed for the represented materials

	Young's modulus (GPa)	Poisson's ratio
25% bone	3.4	0.30
50% bone	6.9	0.30
75% bone	10.3	0.30
100% bone	13.7	0.30
Cortical bone*	13.7	0.30
Cancellous bone*	1.4	0.30
Titanium	115	0.35

*Available only for control models (CM).

attempt to clarify the stress distribution using an FEA model representing complex 3D bone structures *in vivo* around an osseointegrated implant.

Stress distribution in our CM was in accord with the results of other reports where 100% bone-to-implant contact was assumed (Clelland *et al.*, 1991, 1995; Meijer *et al.*, 1993). Inherent differences between MM and CM are the 3D representation of the cancellous bone structure around the implant and the elastic properties of bone used in the models. In MM, 3D

computer graphics was used for model construction and elastic properties of elements were calculated in association with bone volume *in vivo* verified for each cubic element. In contrast, CM (100% bone-implant contact model) generally adopted a Young's modulus for cancellous bone 10 times smaller than cortical bone (Table 1) as reported in the literature. Consequently, less stress under loading would be expected in the cancellous bone area. For the MM, the analysis of biomechanics around the peri-implant bone might have been more accurate because the model reflected bone structure *in vivo* (Korioth & Versluis, 1997).

Smaller elements in the MM would make for an even more accurate analysis. However, such analysis would need a model with a larger number of elements. Therefore, the application of 300 μm cubic elements with four element types in the MM in this study is regarded to be valid for FEA representations of bone as far as analysis feasibility is concerned (Sato *et al.*, 1999a).

Poisson's ratios were not changed with the Young's modulus from 25 to 100% bone because of the negligible effect of the change of Poisson's ratios. Moreover, it was shown that the change of Young's

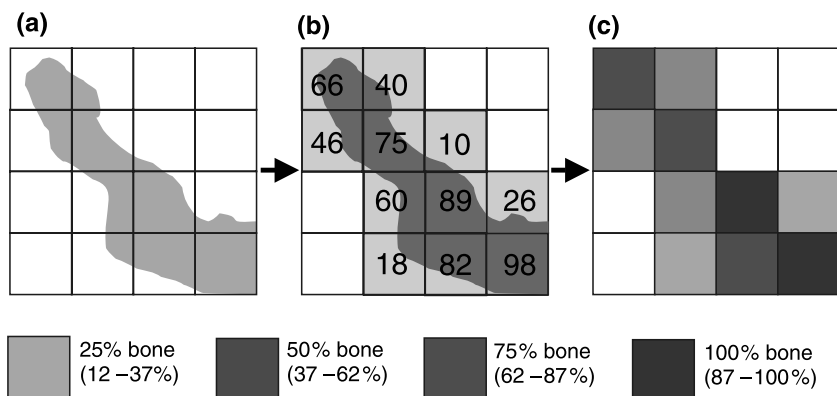


Fig. 2. Mimic model (MM) construction procedure with four categories of 300 μm cubic elements. (a) Cubic grid was superimposed on the 3D graphics, (b) Bone volume (%) was calculated (indicated in each box) and four categories of elements were assigned according to the bone volume, (c) Constructed model.

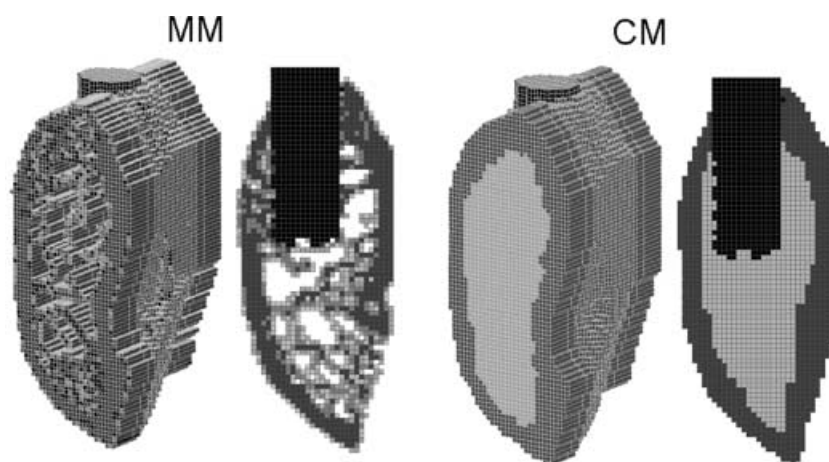


Fig. 3. Oblique view and bucco-lingual central plane of mimic model (MM) and control model (CM). Four kinds of bone brightness in MM correspond to the four categories of elements in Fig. 2.

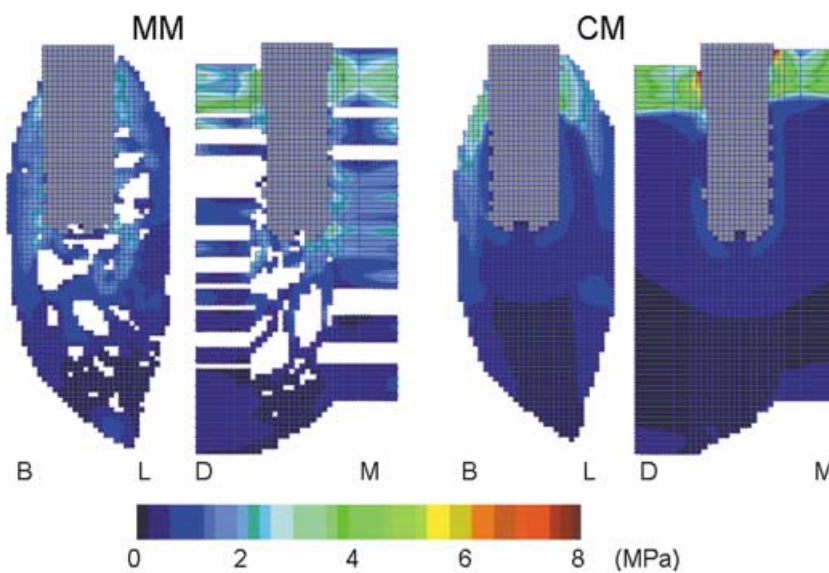


Fig. 4. von Mises stress distribution around the implant in mimic model (MM) and control model (CM). B: buccal, L: lingual, M: mesial, D: distal.

modulus with constant Poisson's ratios resulted in better representation of cancellous bone structures (Sato *et al.*, 1999a).

The effect of bone-implant contact ratio at the bone-implant interface on the stress distribution in the peri-implant bone has been argued (Spivey *et al.*, 1993; Papavasiliou *et al.*, 1997). Higher percentages of theoretically assumed bone-implant contact generated a marked reduction of stresses in the peri-implant bone (Spivey *et al.*, 1993). In contrast, the degree of osseointegration did not affect stress distributions by FEA (Papavasiliou *et al.*, 1997). This controversy may be the result of bone model structures. Therefore, the use of this mimic FEA model simulating the whole structure of the peri-implant cancellous bone might be useful for clarifying the effect of bone-implant contact ratio.

Based on the findings of this limited study, it is concluded that the stress distributions obtained in the new mimic model and the control model were obviously different and the significance of such information will be clarified in future studies.

Acknowledgments

This work was supported partly by Grant-in-Aid for Scientific Research no. 09470437 from the Ministry of Education, Science, Sports and Culture, Japan.

References

- AKAGAWA, Y., WADAMOTO, M., SATO, Y. & TSURU, H. (1992) The three-dimensional bone interface of an osseointegrated implant: a method for study. *Journal of Prosthetic Dentistry*, **68**, 813.
- ALBREKTSSON, T. (1983) Direct bone anchorage of dental implants. *Journal of Prosthetic Dentistry*, **50**, 255.
- BRÄNEMARK, P.-I., ZARB, G.A. & ALBREKTSSON, T. (1987) *Tissue-Integrated Prosthesis. Osseointegration in Clinical Dentistry*, 1st edn, pp. 155. Quintessence, Chicago.
- CLELLAND, N.L., ISMAIL, Y.H., ZAKI, H.S. & PIPKO, D. (1991) Three-dimensional finite element analysis in and around the screw-vent implant. *International Journal of Oral Maxillofacial Implants*, **6**, 391.
- CLELLAND, N.L., LEE, J.K., BIMBENET, O.C. & BRANTLEY, W.A. (1995) A three-dimensional finite element analysis of angle abutments for an implant placed in the anterior maxilla. *Journal of Prosthodontics*, **4**, 95.
- HOLMES, D.C., GRISBY, W.R., GOEL, V.K. & KELLER, J.C. (1992) Comparison of stress transmission in the IMZ implant system with polyoxymethylene or titanium intramobile element: a finite element stress analysis. *International Journal of Oral Maxillofacial Implants*, **7**, 450.
- HOLMES, D.C., HAGANMAN, C.R. & AQUILINO, S.A. (1994) Deflection of superstructure and stress concentrations in the IMZ implant system. *International Journal of Prosthodontics*, **7**, 239.
- HOSHAW, S.J., BRUNSKI, J.B. & COCHRAN, G.V.B. (1994) Mechanical loading of Brånemark implants affects interfacial bone modeling and remodeling. *International Journal of Oral Maxillofacial Implants*, **9**, 345.
- KORIOTH, T.W.P. & VERSLUIS, A. (1997) Modeling the mechanical behavior of the jaws and their related structures by finite element (FE) analysis. *Critical Review of Oral Biology and Medicine*, **8**, 90.
- MEIJER, H.A., STARMANS, F.M., STEEN, W.A. & BOSMAN, F. (1993) A three-dimensional finite element analysis of bone around dental implants in an edentulous human mandible. *Archives of Oral Biology*, **38**, 491.
- MEIJER, H.A., STARMANS, F.M., STEEN, W.A. & BOSMAN, F. (1994) Location of implants in the interforaminal region of the mandible and the consequences for the design of the superstructure. *Journal of Oral Rehabilitation*, **21**, 47.
- MIDDLETON, J., JONES, M.L. & PANDE, G.N. (1996) *Computer Methods in Biomechanics and Biomedical Engineering*, 1st edn, pp. 125. Gordon and Breach Science, Amsterdam.
- PAPAVASILIOU, G., KAMPOSIOIRA, P., BAYNE, S.C. & FELTON, D.A. (1997) 3D-FEA of osseointegration percentages and patterns on implant-bone interfacial stresses. *Journal of Dentistry*, **25**, 485.
- SATO, Y., TEIXEIRA, E.R., TSUGA, K. & SHINDOI, N. (1999a) The effectiveness of a new algorithm on a three-dimensional finite element model construction of bone trabeculae in implant biomechanics. *Journal of Oral Rehabilitation*, **26**, 640.
- SATO, Y., WADAMOTO, M., TSUGA, K. & TEIXEIRA, E.R. (1999b) The effectiveness of element downsizing on a three-dimensional finite element model of bone trabeculae in implant biomechanics. *Journal of Oral Rehabilitation*, **26**, 288.
- SPIVEY, J.D., KONG, W., FOTOS, P.G. & GOEL, W.K. (1993) Stress distribution at the bone-to-implant interface: a 3D finite element analysis. *Journal of Dental Research*, **72**, 117.
- TEIXEIRA, E.R., SATO, Y., AKAGAWA, Y. & SHINDOI, N. (1998) A comparative evaluation of mandibular finite element models with different lengths and elements for implant biomechanics. *Journal of Oral Rehabilitation*, **25**, 299.
- WADAMOTO, M., AKAGAWA, Y., SATO, Y. & KUBO, T. (1996) The three-dimensional bone interface of an osseointegrated implant. I: a morphometric evaluation in initial healing. *Journal of Prosthetic Dentistry*, **76**, 170.

Correspondence: Yuuji Sato, Department of Geriatric Dentistry, Showa University School of Dentistry, 2-1-1, Kitasenzoku, Ohta-ku, Tokyo 145-8515, Japan.
E-mail: sato@senzoku.showa-u.ac.jp.